A photovoltaic pn junction micro vertical comb-drive actuator

2010 J. Micromech. Microeng. 20 105014

(http://iopscience.iop.org/0960-1317/20/10/105014)

J. Micromech. Microeng. **20** (2010) 105014 (8pp) doi:10.1088/0960-1317/20/10/105014

A photovoltaic pn junction micro vertical comb-drive actuator

Hsin-Yu Huang[1], Hsiu-Ting Hsu[2], Hung-Yi Lin[3], Yi Chiu[4] and Weileun Fang[1,2,5]

[1] Department of Power Mechanical Eng., National Tsing Hua University, Hsinchu, Taiwan, Republic of China
[2] Institute of NanoEngineering and MicroSystems, National Tsing Hua University, Hsinchu, Taiwan, Republic of China
[3] Touch Micro-system Technology Corporation, Taoyuan, Taiwan, Republic of China
[4] Department of Electrical Eng., National Chiao Tung University, Hsinchu, Taiwan, Republic of China

E-mail: fang@pme.nthu.edu.tw

Received 7 April 2010, in final form 5 August 2010
Published 9 September 2010
Online at stacks.iop.org/JMM/20/105014

Abstract
This study reports a novel micro electrostatic vertical comb-drive actuator (VCA) driven by the photovoltaic effect that results from incident light. The vertical comb electrodes have a pn junction structure (named pn-combs). The VCA with pn-combs can be driven by the photovoltaic effect. The combination of the photovoltaic effect and reverse bias can further increase the driving amplitude of the VCA. To demonstrate the feasibility of the proposed concept, the VCA with pn-combs was fabricated on an epitaxial silicon wafer (epi-wafer) and successfully driven resonantly by intensity-modulated laser light. The first torsional mode of a typical fabricated VCA is at 1.46 kHz. Moreover, VCA driven using (1) optical driving, and (2) optical driving with dc reverse bias, were also demonstrated. The angular displacement of the VCA was ±3.8 m deg by optical driving. The angular displacement of the VCA significantly increased to ±41 m deg after applying an additional dc reverse bias of 5 V.

(Some figures in this article are in colour only in the electronic version)

1. Introduction

The electrostatic micro vertical comb-drive actuator (VCA) has been extensively used in out-of-plane torsional motion for MEMS applications such as micro-scanning mirrors [1], adaptive optics [2] and optical switches [3]. It has the advantages of large deflection angles, low power consumption, high operation speed and design flexibility. Compared to the gap-closing electrostatic torsional actuator [4], the VCA exhibits no pull-in effect and has large electrostatic force and room for displacement owing to the minimization of gap spacing between fixed and movable combs by incorporating self-aligned techniques.

The VCAs are driven by the electrostatic force due to the asymmetric electric field distribution between the fixed and movable combs. Accordingly, the comb design of the VCAs can be divided into five types. First, a staggered comb design in the early version of VCAs used the device and the handle layers of an SOI wafer to develop the comb electrodes [5]. Second, in the etched-offset comb design of the BELST II process [6], one wet etching and three DRIE processes were employed to fabricate vertical comb electrodes with height offset. Third, the vertical electrodes offset can be achieved by a postprocess assembly such as the selective stiction process [7], residual stress technique [8] or reflow of photoresist [9]. Fourth, the starting electrode [1, 10] was patterned on the in-plane comb structures to break the out-of-plane symmetry of the electric field and resonance can be excited with a relatively small applied voltage. Finally, the pn-based vertical comb electrodes [11] were designed on the pn junctions and driven by reverse electric bias.

All the aforementioned VCAs were driven by applying voltage between fixed and movable electrodes using electrical interconnection. Alternatively, optical actuation is another driving method for micro actuators such as optically controlled silicon cantilever beams [12, 13] and optically actuated MEMS

[5] Author to whom any correspondence should be addressed.

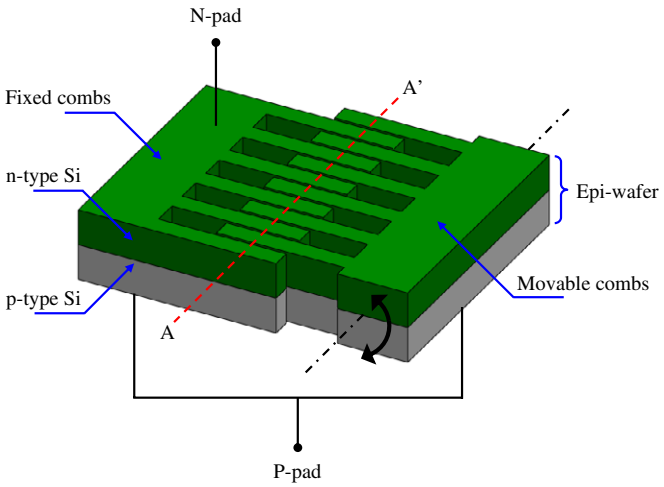

Figure 1. Schematic illustration of the proposed pn-combs actuator.

mirror [14]. However, these micro optical actuators were in fact driven by electric bias in an optically triggered circuit. Directly converting optical energy to mechanical energy in the VCAs was rarely addressed. This study reports a novel approach to drive a VCA optically. A VCA with pn-combs on an epitaxial silicon wafer (epi-wafer) was designed and implemented. In addition to electrical driving, we demonstrate that this VCA can be driven by the direct photovoltaic effect. The details of the VCA with pn-combs are discussed and verified in this study.

2. Concept and design

As the schematic illustration in figure 1 shows, the pn-combs actuator demonstrated in this study consists of fixed combs and movable combs in an epi-wafer. The upper part of pn-combs is n-type silicon; the lower part is p-type silicon. The n-type silicon on the fixed combs is connected to a bonding pad (named N-pad), and the entire p-type silicon is connected to another bonding pad (named P-pad). With a laser light illuminating the fixed as well as the movable combs, or with a voltage applied between the N-pad and P-pad, the pn-combs could be driven into motion by the electrostatic force. Figure 2 shows the cross-section view of AA′ in figure 1. Figure 2(*a*) indicates the concept of optical driving by the photovoltaic effect with light illumination on the fixed combs. The incident light generates photo electron–hole pairs in the pn junction of the fixed combs. According to the photovoltaic effect, a voltage is developed across the pn junction with the p-side positive with respect to the n-side. Here, the open-circuit photovoltaic voltage (V_{PV}) is given by [15]

$$V_{\mathrm{PV}} = \frac{nkT}{q} \ln\left(\frac{I_L}{I_s} + 1\right), \tag{1}$$

where n is the ideality factor, k is the Boltzmann constant, T is the absolute temperature, q is the electronic charge, I_L is the photocurrent and I_s is the saturation current. The photogenerated holes can be distributed in the p-type neutral regions of both fixed and movable combs through the common

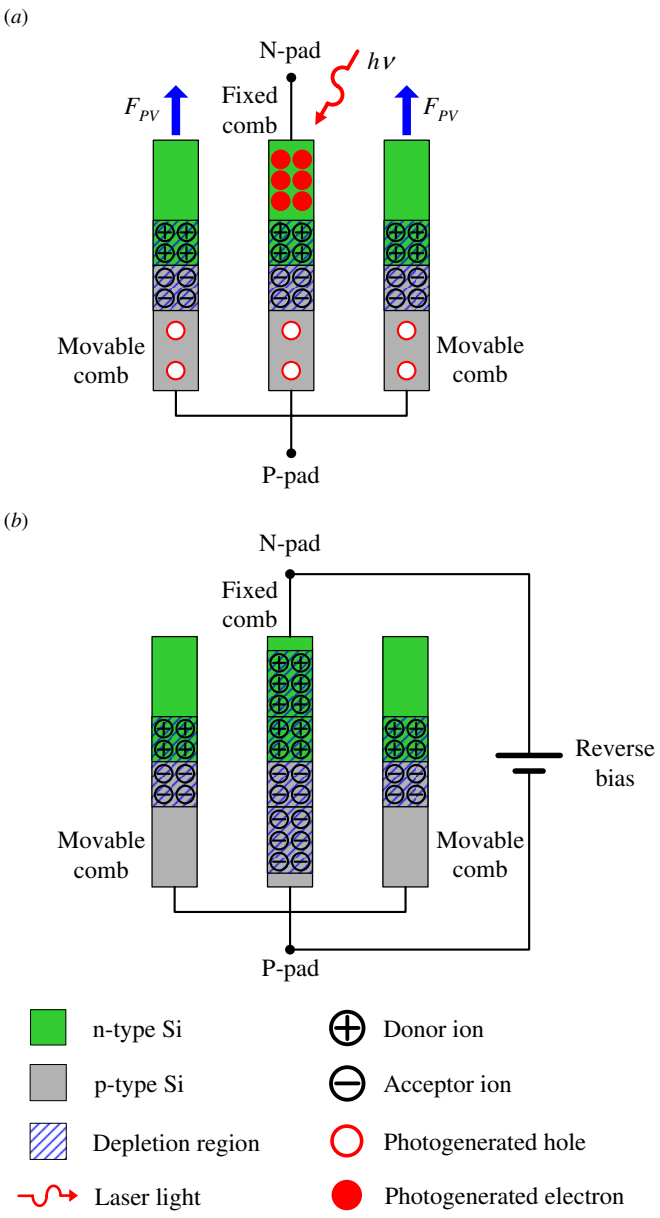

Figure 2. Driving principles of the pn-combs, (*a*) optical driving by the photovoltaic effect, and (*b*) electrical driving by applying a reverse bias.

substrate, whereas the electrons are distributed only in the isolated n-type neutral region of the fixed combs. Therefore, the non-uniform charge distribution generates an asymmetric electrical field and causes a net electrostatic force (F_{PV}) between the fixed and movable combs. The light intensity can be modulated to induce a periodic electrostatic force from this photovoltaic effect to drive the actuator. At mechanical resonance, the pn-combs can have large displacement with relatively small excitation.

Figure 2(*b*) illustrates the electrical driving by applying a reverse bias voltage on the n-type region of the fixed combs (N-pad) while the p-type regions of both fixed and movable combs are connected to ground through the common substrate (P-pad). The reverse bias drops mainly across the depletion region around the metallurgical junctions of the pn-combs.

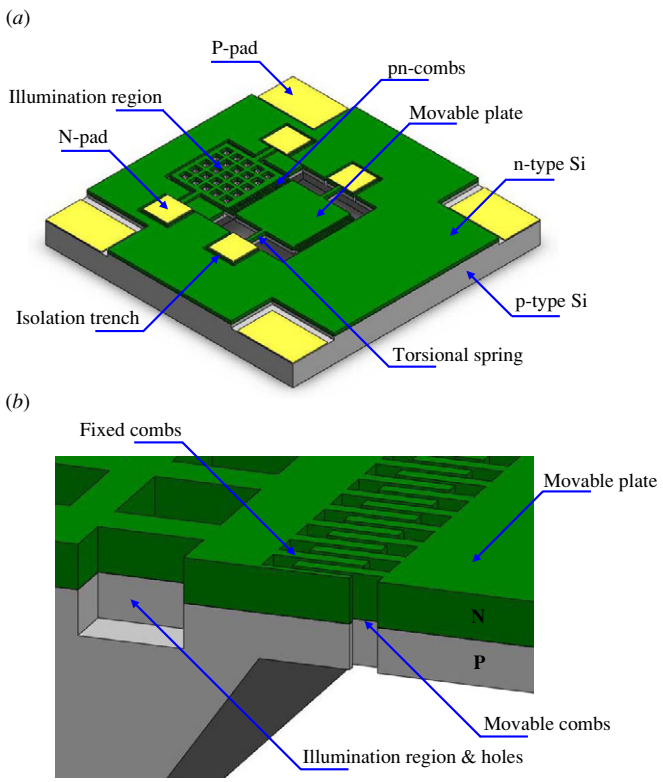

Figure 3. Schematic diagram of (*a*) an angular movable plate consisting of the proposed VCA, and (*b*) zoom-in of the pn-combs and illumination region.

As the depletion region becomes wider and more donor and acceptor ions are exposed, an electrostatic potential is developed between the pn-combs. Since the n-type region of the fixed combs is connected to a fixed potential and that of the movable combs floats, the electrostatic boundary condition is asymmetric, which in turn causes an asymmetric potential and electrostatic field distribution between the combs to actuate the pn-combs. Furthermore, the combination of the photovoltaic effect and the reverse bias can further increase the displacement of the actuator.

Figure 3 shows the schematic diagrams of the VCA to demonstrate the proposed concept. Such a VCA is designed and implemented on a p-type silicon substrate with an n-type epitaxial silicon layer (i.e. epi-wafer). As indicated in figure 3(*a*), the VCA consists of movable pn-combs connected to a movable plate, fixed pn-combs connected to an illumination region, torsional springs, N-pads and P-pads. The movable plate is anchored to the substrate by the torsional springs. The periodical square holes (named illumination holes) in the illumination region are designed to expose the pn junctions so as to increase the illumination area, as indicated in the zoom-in illustration in figure 3(*b*). The fixed pn-combs connected to the illumination region and the movable pn-combs connected to the movable plate are also observed in figure 3(*b*). With the light incident on the illustration region, a photovoltaic voltage is generated between the pn-comb pairs to drive the movable plate. The isolation trenches, as indicated in figure 3(*a*), are employed for electrical isolation between components. Thus, the VCA, the illumination region and their bonding pads (N-pads) are respectively insulated from the surrounded n-type epitaxial silicon layer.

Table 1. Detailed dimensions of a typical VCA with pn-combs design.

Component	Dimension
Torsional springs	400 μm × 12 μm × 30 μm
Movable plate	1500 μm × 1500 μm × 30 μm
Comb fingers	104 μm × 5 μm × 30 μm
Overlap comb length	100
Gap between combs	3 μm
Number of comb pairs (single side actuation)	93
Illumination region	1500 μm × 1500 μm
Illumination holes	50 μm × 50 μm
Illumination hole pitch	50 μm
Isolation trench width	5 μm

3. Fabrication and results

Figure 4 shows the BB′ cross-section of the device fabricated by a four-mask process. To enlarge the thickness of the depletion region, the device was fabricated on an epi-wafer. As shown in figure 4(*a*), the (1 0 0) epi-wafer had a 15 μm thick n-type (7 Ω cm) silicon epitaxial layer on top of a 400 μm thick p-type (20 Ω cm) silicon substrate. As shown in figure 4(*b*), after a Si_xN_y layer (150 nm) was deposited on the wafer by low pressure chemical vapor deposition (LPCVD), the backside Si_xN_y layer was patterned to define the etching window for the subsequent backside wet etching. After the topside Si_xN_y was removed by reactive ion etching (RIE), as illustrated in figure 4(*c*), the patterned photoresist (PR) layer was used as the mask for the following n-type Si etching. After the n-type Si layer was removed by deep reactive ion etching (DRIE), the p-type Si substrate underneath was exposed. As depicted in figure 4(*d*), a lift-off process was employed to pattern a 500 nm thick evaporated Al layer for N-pads and P-pads. To obtain the ohmic contact, the evaporated Al film was annealed at 450 °C for 30 min in N_2 ambient. As illustrated in figure 4(*e*), a 500 nm thick SiO_2 layer was deposited onto the topside of the epi-wafer by plasma-enhanced chemical vapor deposition (PECVD). The SiO_2 layer was then patterned as the hard mask for the following topside DRIE. As shown in figure 4(*f*), a time-controlled anisotropic wet etching was employed to define the thickness of the p-type Si layer (15 μm in this study) for the pn-combs. As indicated in figure 4(*g*), the substrate was patterned by a DRIE process to release the VCA and also define the depth of the illumination holes and the isolation trenches. Thus, both fixed and movable electrodes of the pn-combs can be simultaneously defined using a single mask for a self-aligned process [1, 10, 16]. Finally, as shown in figure 4(*h*), the SiO_2 hard mask was removed by Silox Vapox III solution which has an extremely low etching rate on Al film. The detailed dimensions of the prototype device are summarized in table 1.

Figure 5 shows scanning electron microscope (SEM) micrographs of a typical fabricated VCA with pn-combs. Figure 5(*a*) shows the front side view of the whole device

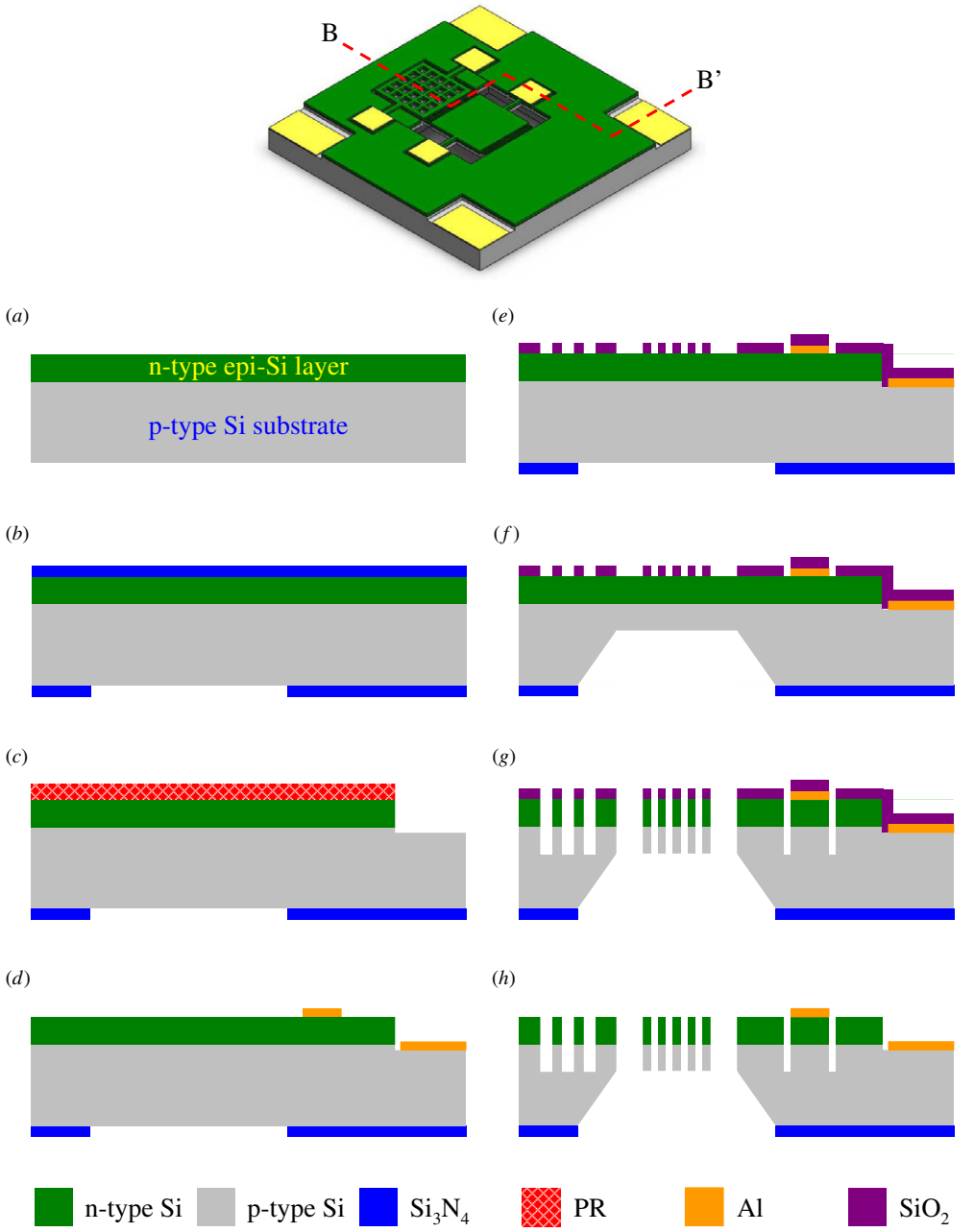

Figure 4. Fabrication process steps (at the cross-section of BB′) of the VCA with pn-combs, (*a*) starting epi-wafer, (*b*) patterning the backside of LPCVD Si_xN_y for wet etching mask, (*c*) patterning the topside cavities for P-pad by DRIE, (*d*) patterning the Al layer for N-pads and P-pads by the lift-off process, and then sintering for ohmic contacts, (*e*) patterning the topside PECVD SiO_2 for a DRIE hard mask, (*f*) etching the backside p-type silicon by KOH solution, (*g*) patterning the substrate by DRIE to release the VCA and also define the depth of the illumination holes and isolation trenches, and (*h*) removing the SiO_2 mask by Silox Vapox III solution.

consisting of the VCA and the illumination region. The pn-combs, N-pads, P-pads and isolation trenches can also be observed. The geometry as well as the stiffness of the torsional springs can be easily controlled by the process. Figure 5(*b*) shows a backside view of the device, in which the bulk-etched cavity of the VCA is observed. Figure 5(*c*) further shows a zoom-in of the illumination region with illumination holes and pn-combs. The zoom-in micrograph in figure 5(*d*) shows the fixed pn-combs on the illumination region and the movable pn-combs on the movable plate. As shown in figure 5(*e*), the N-pad and its isolation trench can be observed. Finally, the cross-section of the movable plate in figure 5(*f*) shows the pn junction profile observed by the copper-staining method [17].

4. Testing

Various tests have been performed to demonstrate the presented concept. The test setup in figure 6(*a*) was established to characterize the dynamic behavior of the VCA driven optically with or without a dc reverse bias. The laser is incident onto the illumination region to drive the VCA optically; the

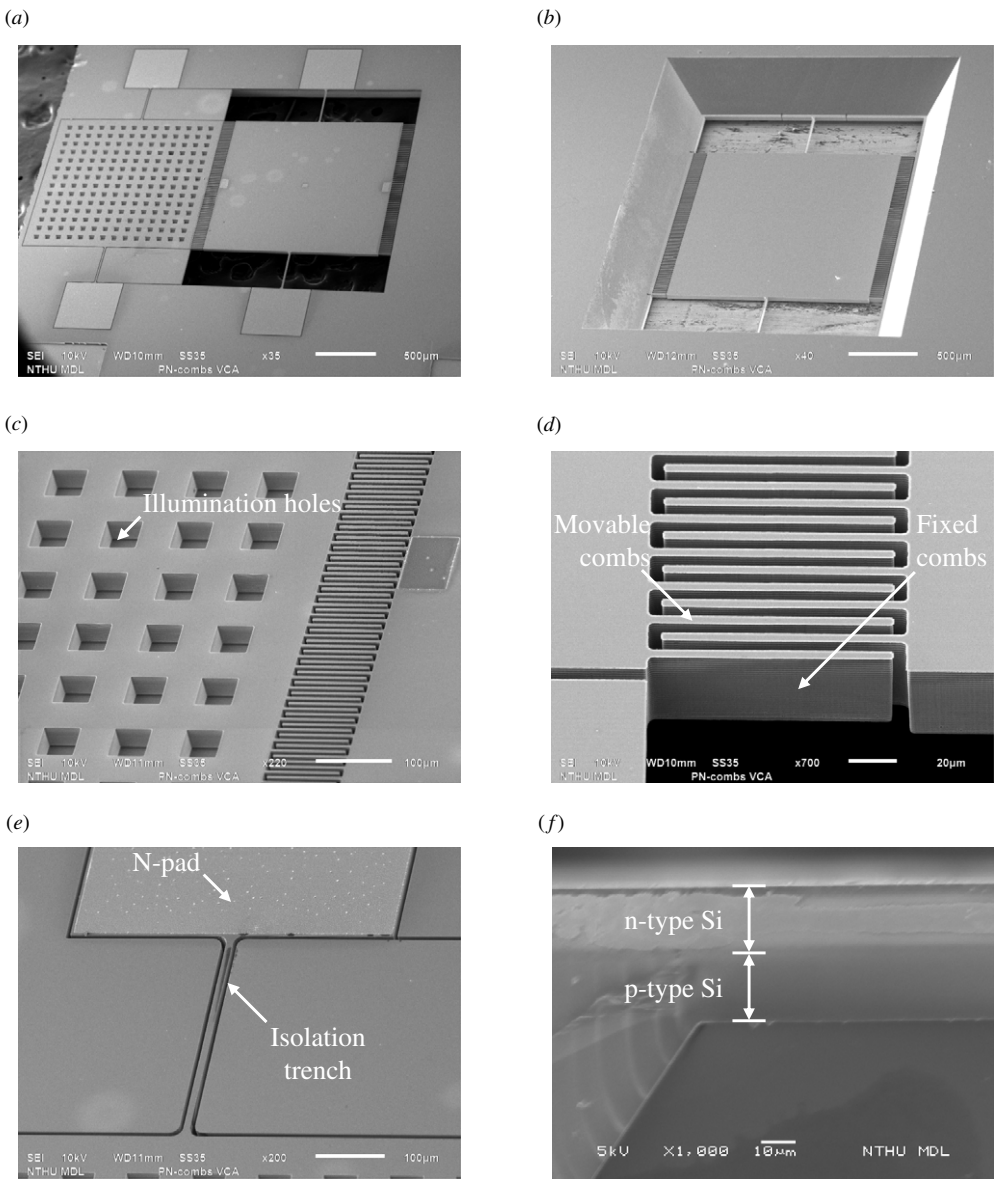

Figure 5. SEM micrographs of a typical fabricated VCA with pn-combs: (*a*) front side view, (*b*) backside view, zoom-in of (*c*) illumination region with illumination holes and pn-combs, (*d*) fixed and movable pn-combs, (*e*) N-pad and its isolation trench, and (*f*) cross-section of the movable plate.

laser intensity is modulated on and off periodically by a function generator. As the VCA is under optical driving, an additional dc reverse bias can be further applied to the fixed combs. The dynamic response of the VCA was measured by a commercial LDV (laser Doppler vibrometer). The optical micrograph in figure 6(*b*) shows a typical device under test. The probes were used to apply a reverse bias through the N-pad and P-pad, and the observed laser spot was reflected from the incident laser beam.

Figure 7 shows the electrical measurement of the VCA with pn-combs. As indicated in figure 6, a laser diode of 650 nm wavelength and 3.4 mW power was projected to the illumination region and the current–voltage (*I–V*) characteristic was measured using a source meter and a probe station. An equivalent circuit is shown in figure 7(*a*). It consists of a pn junction and a series resistance R_s of the neutral region of the p-type substrate and the n-type epitaxial layer. The R_s was measured between two N-pads or two P-pads to be about 1 MΩ. This high resistance is due to the high resistivity of the substrate and the epitaxial layer. Without illumination, a rectifying characteristic was observed with a saturation current of 0.36 μA at reverse bias. When the laser illuminates the device, a clear photocurrent $I_{\mathrm{ph}} = 72$ μA can be seen in figure 7(*b*). The photocurrent depends on the incident laser intensity, as observed during the tests. Therefore the photovoltaic effect in the fabricated device is verified. However, figure 7(*b*) also shows some non-ideality in the IV curve. The diode does not have a clear turn-on voltage at forward bias. Under illumination, the device also shows ohmic behavior for smaller reverse bias. These non-idealities can be attributed to potential causes such as (1) high resistivity of the

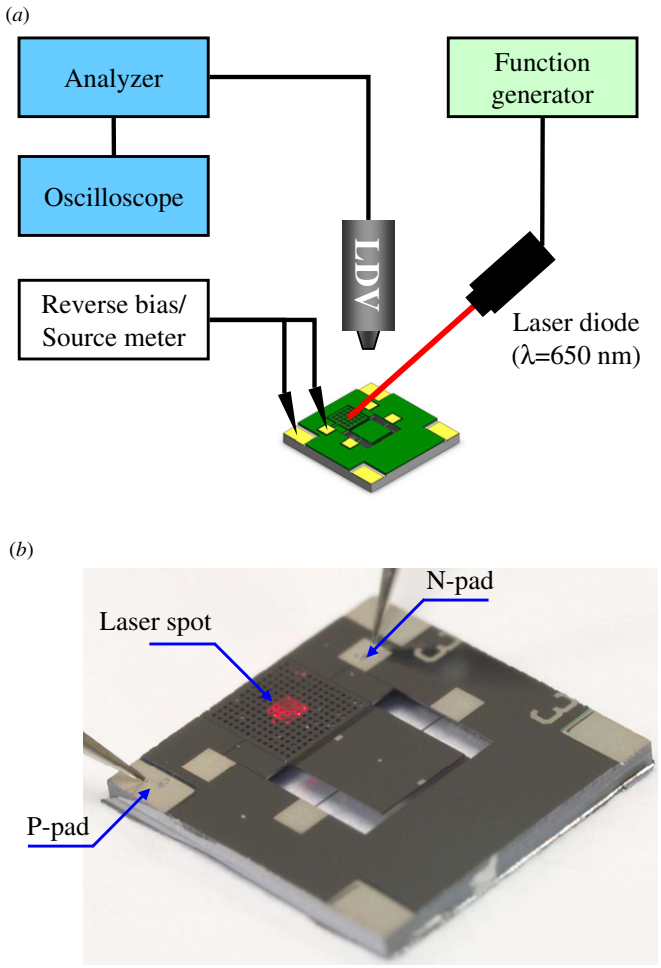

Figure 6. (*a*) Test setup to characterize the pn-combs and the VCA, and (*b*) optical micrograph of a typical device under test.

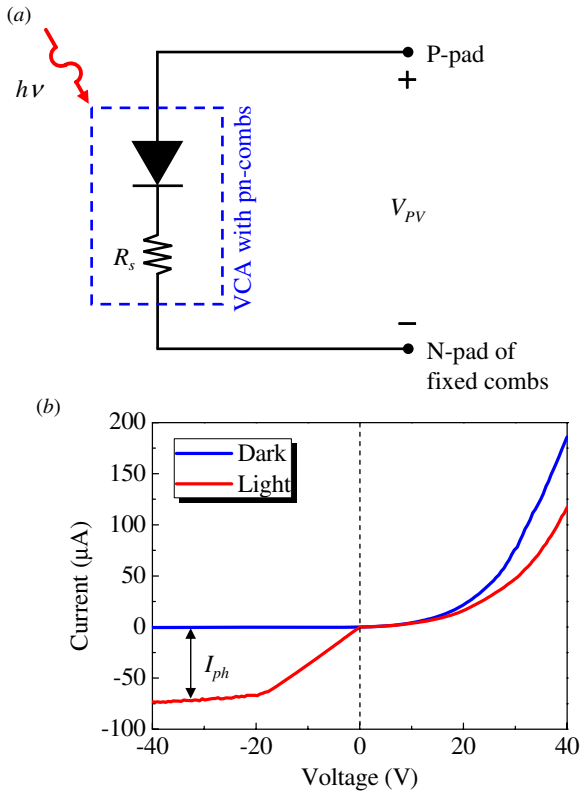

Figure 7. Electrical measurement of the VCA with pn-combs, (*a*) equivalent circuit and (*b*) typical *I*–*V* characteristic of the fabricated pn-combs.

Table 2. Performance of a typical proposed VCA with pn-combs.

Driving method: Optical driving		
Resonant frequency	1.46 kHz	
Driving source	Intensity-modulated laser (650 nm, 3.4 mW)	
Control source	0 V dc (RB)	5 V dc (RB)
Angular displacement (± m deg)	3.8	41

silicon substrate and thus non-ideal ohmic contact between the Al layer and the substrate; (2) surface damage and defect on the exposed side walls of the pn-combs by the DRIE process and (3) other process contamination. Further study is under way to investigate the detailed causes and possible solutions of these phenomena.

The measurements in figure 8 show the VCA driven optically by only applying an incident laser. During the tests, the 650 nm laser diode was switched on and off periodically at various frequencies. Thus, the induced photovoltaic voltage as well as the associated electrostatic force drove the VCA periodically. The time responses in figure 8(*a*) respectively show the 3.3 V_{pp} square wave (top) used to modulate the laser diode, the measured photovoltaic voltage of the pn-combs (middle) and the associated angular displacement of the VCA (bottom). Figure 8(*b*) shows the typical frequency response of the angular displacement of the VCA when driven by such a periodic laser power of 3.4 mW. The first torsional mode is 1.46 kHz with an angular displacement of ±3.8 m deg. Figure 9 further shows the device driven by not only a modulated laser but also a dc reverse bias across the pn junction. The measured frequency responses in figure 9(*a*) show the angular displacement driven by an incident 3.4 mW laser and a 3 V dc reverse bias (RB). Under such excitation conditions, the resonant frequency remains 1.46 kHz with a maximum angular motion of ±31.6 m deg. In comparison, the angular displacement driven by only the laser beam is also shown in figure 9(*a*). In short, the angular displacement of the VCA has been increased by eight-fold by the applied dc reverse bias providing an additional electrostatic force to the pn-combs and thus significantly increasing the angular displacement. The maximum angular displacement of the VCA at its resonant frequency can be further increased by increasing the dc reverse bias, as shown in figure 9(*b*). According to the measurement results, the maximum angular displacement of the VCA became ±41 m deg when the dc reverse bias increased to 5 V.

In short, the VCA was successfully driven by the electrostatic force in the pn-combs induced photovoltaically. The dynamic response of the VCA can also be enhanced by using the photovoltaic effect and the electrical bias simultaneously. Detailed performance of the VCA with

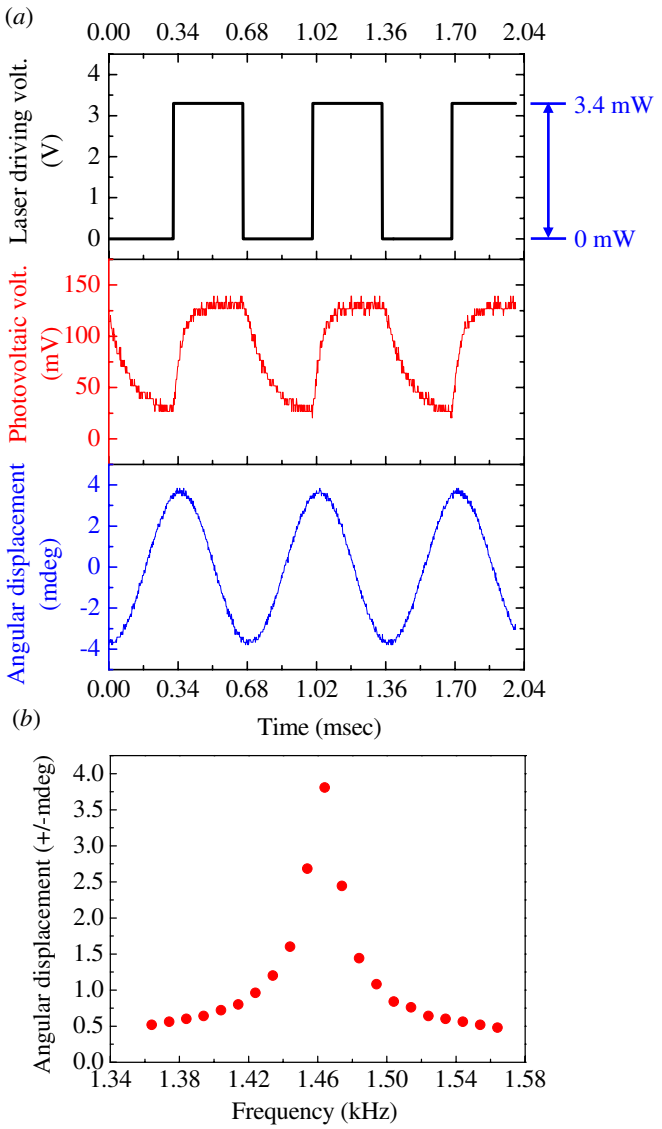

Figure 8. Optical driving, (*a*) time response of the square wave used to modulate the laser diode (top), the measured photovoltaic voltage of the pn-combs (middle), and the associated angular displacement of the VCA (bottom), and (*b*) typical frequency response of the VCA.

pn-combs is summarized in table 2. The testing results demonstrate the feasibility of the proposed VCA with pn-combs.

5. Conclusions

This study has successfully demonstrated a novel micro vertical comb-drive actuator with photovoltaic pn junctions. The four-mask process on the epitaxial silicon wafer facilitates easy fabrication of the self-aligned VCA with pn-combs. The VCA with pn-combs can be driven by the electrostatic force resulted from the photovoltaic effect. Moreover, the driving amplitude of the VCA can be further increased by the dc reverse bias. A ±3.8 m deg angular displacement has been demonstrated by a typical fabricated VCA. The angular displacement of the VCA has been increased to ±41 m deg after applying a 5 V dc reverse bias. The proposed VCA has

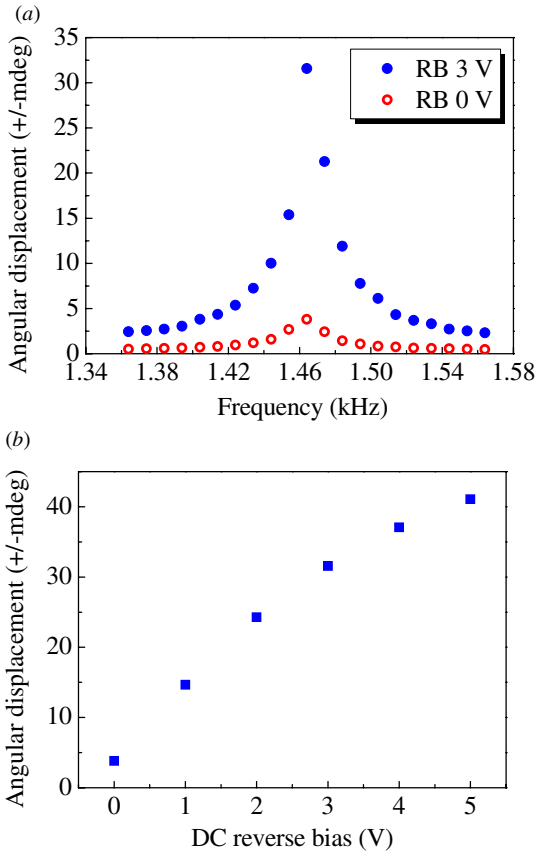

Figure 9. Optical driving with different dc reverse bias (RB), (*a*) frequency response of the VCA driven by incident laser and a 3 V dc reverse bias, (*b*) relationship between the applied dc reverse bias and angular displacement of the VCA at its resonant frequency.

the following advantages and characteristics. First, the self-aligned fabrication processes of the vertical comb electrodes are easy and simple. Second, the photovoltaic effect can be used in the pn-combs to directly convert optical energy to mechanical energy. Third, the combination of the photovoltaic effect and the reverse bias can further increase the angular displacement of the VCA.

Acknowledgments

This study was partially supported by the National Science Council of Taiwan under grant NSC-96-2628-E-007-008-MY3. The authors appreciate the Center for Nanotechnology, Materials Science and Microsystems (CNMM) of National Tsing Hua University, the Nano Facility Center (NFC) of National Chiao Tung University, the National Nano Device Laboratories (NDL) of National Applied Research Laboratories (NARL), and the Nano-Electro-Mechanical-Systems (NEMS) Research Center of National Taiwan University for providing the fabrication facilities.

References

[1] Schenk H, Dürr P, Kunze D, Lakner H and Kück H 2001 A resonantly excited 2D-micro-scanning-mirror with large deflection *Sensors Actuators* A **89** 104–11

[2] Milanović V, Kwon S and Lee L P 2004 High aspect ratio micromirrors with large static rotation and piston actuation *IEEE Photonics Technol. Lett.* **16** 1891–3
[3] Tsai J C and Wu M C 2006 A high port-count wavelength-selective switch using a large scan-angle, high fill-factor, two axis MEMS scanner array *IEEE Photonics Technol. Lett.* **18** 1439–41
[4] Hsieh J and Fang W 2000 A novel microelectrostatic torsional actuator *Sensors Actuators* A **79** 64–70
[5] Conant R A, Nee J T, Lau K Y and Muller R S 2000 A flat high-frequency scanning micromirror *IEEE Solid-State Sensor and Actuator Workshop Technical Digest (Hilton Head Island, SC, 4–8 June 2000)* pp 6–9
[6] Tsai J M-L, Chu H-Y, Hsieh J and Fang W 2004 The BELST II process for a silicon high-aspect-ratio micromaching vertical comb actuator and its applications *J. Micromech. Microeng.* **14** 235–41
[7] Kim J, Christensen D and Lin L 2006 Micro vertical comb actuators by selective stiction process *Sensors Actuators* A **127** 248–54
[8] Jeong K-H and Lee L P 2005 A novel microfabrication of a self-aligned vertical comb drive on a single SOI wafer for optical MEMS applications *J. Micromech. Microeng.* **15** 277–81
[9] Hah D, Patterson P R, Nguyen H D, Toshiyoshi H and Wu M C 2004 Theory and experiments of angular vertical comb-drive actuators for scanning micromirrors *IEEE J. Sel. Top. Quantum Electron.* **10** 505–13
[10] Schenk H, Dürr P, Haase T, Kunze D, Sobe U, Lakner H and Kück H 2000 Large deflection micromechanical scanning mirrors for linear scans and pattern generation *IEEE J. Sel. Top. Quantum Electron.* **6** 715–22
[11] Abu-Ageel N M 2004 Micro-machine electrostatic actuator, method and system employing same, and fabrication methods thereof *US Patent No* 6757092 B2
[12] Tabib-Azar M 1990 Optically controlled silicon microactuators *Nanotechnology* **1** 81–92
[13] Yamauchi Y, Higo A, Kakushima K, Fujita H and Toshiyoshi H 2004 Optically assisted electrostatic actuation mechanism *IEEE/LEOS Int. Conf. on Optical MEMS and Their Applications (Optical MEMS 2004) (Takamatsu, Japan, 22–26 August 2004)* pp 164–5
[14] Yamauchi Y, Higo A, Kakushima K, Fujita H and Toshiyoshi H 2005 A light-in light-out micro mirror device *Digest Tech. Papers Transducers'05 Conf. (Seoul, Korea, 5–9 June 2005)* pp 1175–8
[15] Sze S M and Ng K K 2007 *Physics of Semiconductor Devices* 3rd edn (Hoboken, NJ: Wiley)
[16] Tsou C, Lin W T, Fan C C and Chou B C S 2005 A novel self-aligned vertical electrostatic combdrive actuator for scanning micromirrors *J. Micromech. Microeng.* **15** 855–60
[17] Ahn S T and Tiller W A 1988 A staining technique for the study of two-dimensional dopant diffusion in silicon *J. Electrochem. Soc.* **135** 2370–3